

UCLA

UCLA Previously Published Works

Title

Rocking Response of Free-Standing Blocks Under Cycloidal Pulses

Permalink

<https://escholarship.org/uc/item/24w4q3jx>

Journal

Journal of Engineering Mechanics, 127(5)

Authors

Zhang, Jian

Makris, Nicos

Publication Date

2001

Peer reviewed

ROCKING RESPONSE OF FREE-STANDING BLOCKS UNDER CYCLOIDAL PULSES

By Jian Zhang¹ and Nicos Makris,² Member, ASCE

ABSTRACT: This paper examines in depth the transient rocking response of free-standing rigid blocks subjected to physically realizable trigonometric pulses. First, the expressions for the dynamic horizontal and vertical reactions at the pivot point of a rocking block are derived and it is shown that the coefficient of friction needed to sustain pure rocking motion is, in general, an increasing function of the acceleration level of the pulse. Subsequently, this paper shows that under cycloidal pulses a free-standing block can overturn with two distinct modes: (1) by exhibiting one or more impacts; and (2) without exhibiting any impact. The existence of the second mode results in a safe region that is located on the acceleration-frequency plane above the minimum overturning acceleration spectrum. The shape of this region depends on the coefficient of restitution and is sensitive to the nonlinear nature of the problem. This paper concludes that the sensitive nonlinear nature of the problem, in association with the presence of the safe region that embraces the minimum overturning acceleration spectrum, complicates further the task of estimating peak ground acceleration by only examining the geometry of free-standing objects that either overturned or survived a ground shaking.

INTRODUCTION

Under strong ground shaking, tall, rigid structures might enter into rocking motion that occasionally results in overturning. As examples, Fig. 1 shows electrical equipment at the Sylmar Converter Station that overturned during the 1971 San Fernando earthquake, and Fig. 2 shows the San Francisco-bound train at Point Reyes that overturned during the 1906 San Francisco earthquake. Early studies on the rocking response of a rigid block supported on a base undergoing horizontal motion were presented by Housner (1963). In that study, the base acceleration was represented by a rectangular or a half-sine pulse and expressions were derived for the minimum acceleration amplitude required to overturn the block. Although Housner's pulses are not physically realizable and his solution for the minimum overturning acceleration under a half-sine pulse is unconservative (Shi et al. 1996; Makris and Roussos 1998, 2000), his pioneering work uncovered a scale effect that explained why the larger of two geometrically similar blocks can survive the excitation that will topple the smaller block. Following Housner's seminal paper a large number of studies have been presented to address the complex dynamics of one of the simplest man-made structures—the free-standing block. Yim et al. (1980) adopted a probabilistic approach and conducted a numerical study using artificially generated ground motions to show that the rocking response of a block is sensitive to system parameters. Experimental and analytical studies on the same problem have been reported by Aslam et al. (1980), who confirmed that, under artificially generated motions, the rocking response of rigid blocks is sensitive to the system parameters.

The rocking response of free-standing blocks subjected to harmonic steady-state loading was studied in detail by Spanos and Koh (1984), who identified “safe” and “unsafe” regions and developed analytical methods for determining the fundamental and subharmonic modes of the system. Their study was

extended by Hogan (1989, 1990), who further elucidated the mathematical structure of the problem by introducing the concepts of orbital stability and Poincaré sections. Perhaps, Hogan's finding that is most relevant to earthquake engineering is that the domain of maximum transients of his solutions appears relatively ordered and possesses a high degree of predictability despite the unpredictability that is present in the asymptotic part of the solutions (Hogan 1989). The steady-state rocking response of rigid blocks was also studied ana-

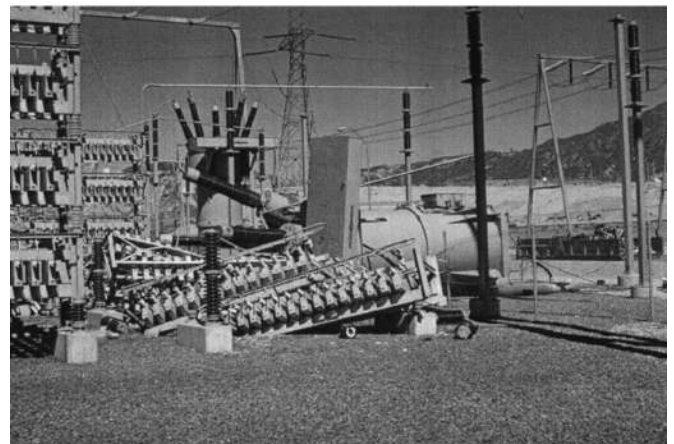


FIG. 1. Overturned Electrical Equipment at Sylmar Converter Station after 1971 San Fernando Earthquake (Top: Front View; Bottom: Side View) (Steinbrugge Collection, Pacific Earthquake Engineering Research Center, University of California, Berkeley)

¹Grad. Res. Asst., Dept. of Civ. and Envir. Engrg., Univ. of California, Berkeley, CA 94720.

²Assoc. Prof., Dept. of Civ. and Envir. Engrg., SEMM, Univ. of California, Berkeley, CA 94720.

Note. Associate Editor: James Beck. Discussion open until October 1, 2001. Separate discussions should be submitted for the individual papers in this symposium. To extend the closing date one month, a written request must be filed with the ASCE Manager of Journals. The manuscript for this paper was submitted for review and possible publication on January 14, 2000; revised September 19, 2000. This paper is part of the *Journal of Engineering Mechanics*, Vol. 127, No. 5, May, 2001. ©ASCE, ISSN 0733-9399/01/0005-0473-0483/\$8.00 + \$.50 per page. Paper No. 22196.

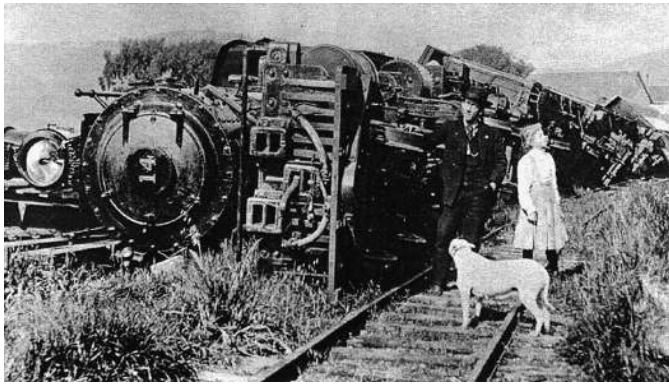


FIG. 2. Overturned Train (San Francisco Bound) at Point Reyes Station during 1906 San Francisco Earthquake (Roy D. Graves Collection)

lytically and experimentally by Tso and Wong (1989a,b). Although their theoretical study was not as in-depth as the one presented by Hogan (1989), their experimental work provided valuable support to theoretical findings. Other related studies are referenced in the above-mentioned papers.

Although the early work of Yim et al. (1980) used artificially generated white-noise-type motions and the work of Spanos and Koh (1984), Hogan (1989, 1990), and Tso and Wong (1989a,b) used long-duration harmonic motions, this paper is redirected to pulse-type motions, which are found to be good representatives of near-source ground motions (Campillo et al. 1989; Iwan and Chen 1994; Makris and Roussos 1998). Herein this study builds on Housner's early work (1963) to investigate the overturning potential of simple trigonometric pulses known as cycloidal pulses (Jacobsen and Ayre 1958). This study examines in-depth the rocking response of a free-standing block to one-sine and one-cosine acceleration pulses. These two trigonometric pulses are physically realizable and resemble in several occasions the fault-parallel and fault-normal component of motions recorded near the source of strong earthquakes (Makris and Roussos 1998, 2000).

This paper reveals that under cycloidal pulses a free-standing block can overturn with two distinct modes: (1) by exhibiting one or more impacts; and (2) without exhibiting any impact. The existence of the second mode results in a safe region that is located over the minimum overturning acceleration spectrum. It is found that the shape of this region depends on the coefficient of restitution and is sensitive to the nonlinear nature of the problem. The transition from mode 1 to mode 2 is sudden and results to a finite jump in the minimum overturning acceleration spectrum. In a recent study, Anooshehpour et al. (1999) attempted to construct minimum overturning acceleration spectra due to a one-sine pulse. Their study was motivated from the temptation to back-figure peak ground accelerations that overturned the locomotive shown in Fig. 2. Unfortunately, their analysis (1) failed to identify the second mode of overturning (without impact) and therefore ignored the presence of the aforementioned safe region; and (2) overlooked the sensitivity of the rocking response to its nonlinear nature. This study addresses these issues in conjunction with the interface condition needed to sustain purely rocking motion.

REVIEW OF ROCKING RESPONSE OF FREE-STANDING BLOCK

Condition for Initiation of Rocking Motion

Consider the rigid block shown in Fig. 3 (top) with slenderness α , which can oscillate about the centers of rotation O and O' when it is set to rocking. Depending on the level and form of the ground acceleration, the block may translate with

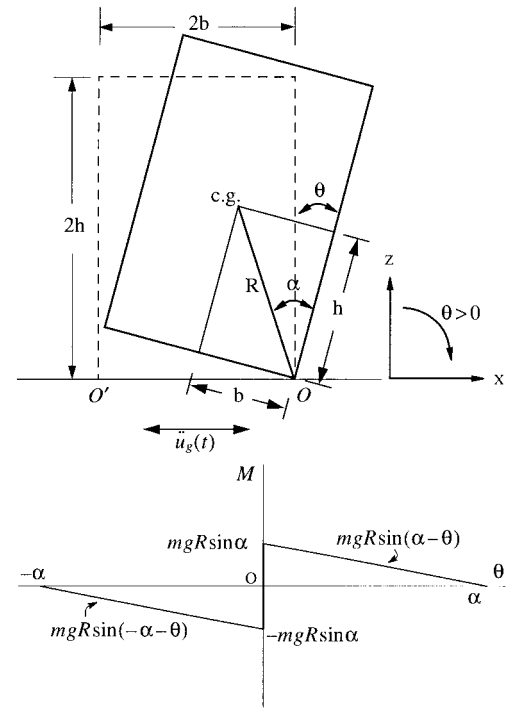


FIG. 3. Schematic of Free-Standing Block in Rocking Motion (Top) and Its Moment Rotation Diagram (Bottom)

the ground, slide, rock, or slide rock. Prior to 1996, the mode of rigid-body motion that prevailed has been determined by comparing the available static friction to the width-to-height ratio of the block, irrespective of the magnitude of the horizontal ground acceleration. At about the same time, Scalia and Sumbatyan (1996) and, independently, Shenton (1996) indicated that, in addition to pure sliding and pure rocking, there is a slide-rock mode and its manifestation depends not only on the width-to-height ratio and the static friction coefficient but also on the magnitude of the base acceleration.

Physically realizable cycloidal pulses have displacement histories that are continuous and differentiable signals that build up gradually from zero. Their corresponding acceleration histories might be zero at the time origin or exhibit a finite value that can be as large as their maximum amplitude. Fig. 4 plots the acceleration, velocity, and displacement histories of a one-sine pulse (left) and one-cosine pulse (right). In the case of the one-sine pulse, the ground acceleration is zero at the initiation of motion and builds up gradually. In contrast, in the case of a one-cosine pulse, the ground acceleration assumes its maximum value at the initiation of motion. Under other cycloidal pulses such as Type- C_n pulses (Makris and Roussos 1998), the ground acceleration is finite at the initiation of motion but assumes a value that is smaller than its maximum amplitude a_p . With reference to Fig. 3 and assuming that the coefficient of friction $\mu > (b/h) = \tan \alpha$, static equilibrium yields that the minimum horizontal acceleration that is needed to initiate rocking is $a_{p,\min} = g \tan \alpha$. Consequently, pulses with amplitude $a_p > g \tan \alpha$ will induce rocking to a rectangular block with slenderness α .

Consider a cycloidal pulse with acceleration amplitude $a_p > g \tan \alpha$, and let λa_p be the value of the ground acceleration when a block with slenderness α is about to enter rocking motion. Depending on the type of pulse, λ assumes different values; however, it is bounded by

$$\frac{g \tan \alpha}{a_p} < \lambda \leq 1 \quad (1)$$

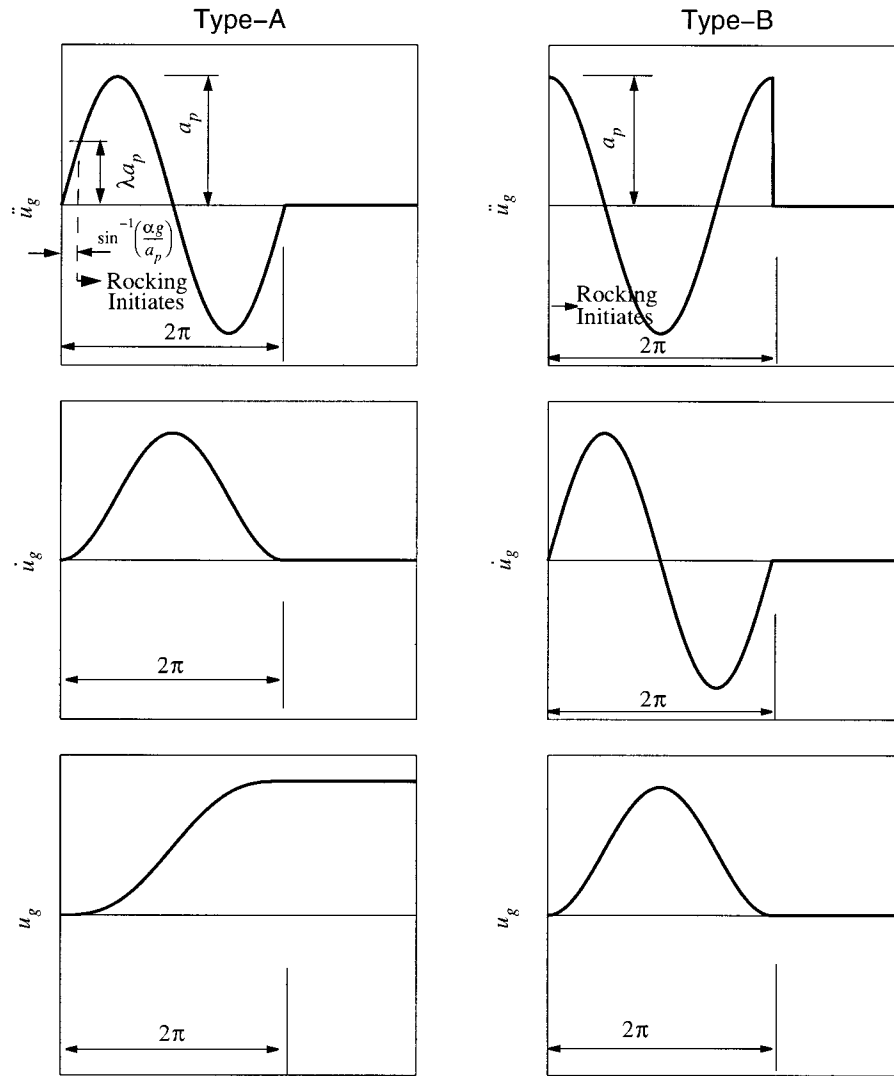


FIG. 4. Acceleration, Velocity, and Displacement Histories of One-Sine Pulse (Left) and One-Cosine Pulse (Right)

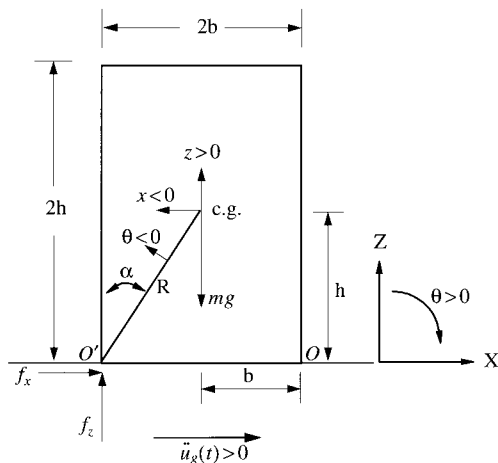


FIG. 5. Free-Body Diagram of Rigid Block at Instant That It Enters Rocking Motion

Fig. 5 shows the free-body diagram of a free-standing block that is about to enter rocking motion due to a positive ground acceleration. With the system of axis shown, a positive acceleration will induce an initial negative rotation ($\theta < 0$). Adopting the notation introduced by Shenton (1996), let $f_x > 0$ and $f_z > 0$ be the horizontal and vertical reactions at the tip O' of the block. Dynamic equilibrium at this instant ($\theta = 0$) gives

$$f_x(0) = m(\lambda a_p + h\ddot{\theta}(0)) \quad (2)$$

$$f_z(0) = m(g - b\ddot{\theta}(0)) \quad (3)$$

$$I_{cg}\ddot{\theta}(0) = -f_x(0)h + f_z(0)b \quad (4)$$

where I_{cg} = moment of inertia of the block about its center of gravity (for rectangular blocks $I_{cg} = mR^2/3$). Substitution of (2) and (3) into (4) gives the value of the angular acceleration $\ddot{\theta}_0$ at the instant when rocking initiates

$$\ddot{\theta}(0) = \ddot{\theta}_0 = -p^2 \sin \alpha \left(\frac{\lambda a_p}{g \tan \alpha} - 1 \right) \quad (5)$$

in which $p = \sqrt{3g/(4R)}$ = frequency parameter of the block (rad/s); whereas $R = \sqrt{b^2 + h^2}$ = half-diameter of the block—a measure of its size. To avoid sliding at this instant ($t = 0$)

$$\frac{f_x(0)}{f_z(0)} \leq \mu \quad (6)$$

and substitution of the value computed by (5) into (2) and (3) gives the condition for a block to enter the rocking motion without sliding

$$\frac{\lambda a_p - \frac{3}{4} g \cos \alpha \sin \alpha \left(\lambda \frac{a_p}{g \tan \alpha} - 1 \right)}{g + \frac{3}{4} g \sin^2 \alpha \left(\lambda \frac{a_p}{g \tan \alpha} - 1 \right)} \leq \mu \quad (7)$$

Eq. (7), initially presented by Shenton (1996) and subsequently by Pompei et al. (1998), indicates that, under some excitation pulses with amplitude a_p , the condition for a block to enter rocking motion without sliding depends on the value of a_p . However, this is true only for pulses that have a finite acceleration at the initiation of motion. For pulses in which acceleration history builds up gradually (such as a one-sine pulse), the value of λa_p at the initiation of rocking is equal to $g \tan \alpha$ and (7) reduces to

$$\tan \alpha = \frac{b}{h} \leq \mu \quad (8)$$

which is the traditional expression that one derives from static analysis. Once the block enters rocking motion, the horizontal reaction $f_x(t)$ and vertical reaction $f_z(t)$ fluctuates with time. Consequently, to avoid sliding during the entire duration of the rocking motion

$$\left| \frac{f_x(t)}{f_z(t)} \right| < \mu \quad \text{at all times} \quad (9)$$

This dynamic condition is investigated in the subsequent section, because it involves the time histories of the angular acceleration and the angular velocity.

Governing Equations under Rocking Motion

Under a positive horizontal ground acceleration and assuming that the coefficient of friction is large enough so that there is no sliding, the block will initially rotate with a negative rotation, $\theta < 0$, and, if it does not overturn, it will eventually assume a positive rotation, and so forth. The equations that govern this motion are

$$I_0 \ddot{\theta}(t) + mgR \sin[-\alpha - \theta(t)] = -m\ddot{u}_g(t)R \cos[-\alpha - \theta(t)], \quad \theta(t) < 0 \quad (10)$$

$$I_0 \ddot{\theta}(t) + mgR \sin[\alpha - \theta(t)] = -m\ddot{u}_g(t)R \cos[\alpha - \theta(t)], \quad \theta(t) > 0 \quad (11)$$

Eqs. (10) and (11) are well known in the literature (Yim et al. 1980) and are valid for arbitrary values of the angle $\alpha = \text{atan}(b/h)$. For rectangular blocks, $I_0 = (4/3)mR^2$, (10) and (11) can be expressed in the compact form

$$\ddot{\theta}(t) = -p^2 \left\{ \sin[\alpha \text{sgn}[\theta(t)] - \theta(t)] + \frac{\ddot{u}_g}{g} \cos[\alpha \text{sgn}[\theta(t)] - \theta(t)] \right\} \quad (12)$$

The oscillation frequency of a rigid block under free vibration is not constant, because it strongly depends on the vibration amplitude (Housner 1963). Nevertheless, the quantity p is a measure of the dynamic characteristics of the block. For an electrical transformer, $p \approx 2$ rad/s, and for a household brick, $p \approx 8$ rad/s.

Fig. 3 (bottom) shows the moment-rotation relationship during the rocking motion of a free-standing block. The system has infinite stiffness until the magnitude of the applied moment reaches $mgR \sin \alpha$, and once the block is rocking, its stiffness decreases monotonically, reaching zero when $\theta = \alpha$. During the oscillatory rocking motion, the moment-rotation curve follows this curve without enclosing any area. Energy is lost only during impact, when the angle of rotation reverses. When the angle of rotation reverses, it is assumed that the rotation continues smoothly from points O to O' . Conservation of momentum about point O' just before the impact and right after the impact gives

$$I_0 \dot{\theta}_1 - m\dot{\theta}_1 2bR \sin(\alpha) = I_0 \dot{\theta}_2 \quad (13)$$

where $\dot{\theta}_1$ = angular velocity just prior to the impact; and $\dot{\theta}_2$ = angular velocity right after the impact. The ratio of kinetic energy after and before the impact is

$$r = \frac{\dot{\theta}_2^2}{\dot{\theta}_1^2} \quad (14)$$

which means that the angular velocity after the impact is only \sqrt{r} times the velocity before the impact. Substitution of (14) into (13) gives

$$r = \left[1 - \frac{3}{2} \sin^2 \alpha \right]^2 \quad (15)$$

The value of the coefficient of restitution given by (15) is the maximum value of r under which a block with slenderness α will undergo rocking motion. Consequently, to observe rocking motion, the impact has to be inelastic. The less slender a block (larger α), the more plastic is the impact, and for the value of $\alpha = \sin^{-1} \sqrt{2/3} = 54.73^\circ$, the impact is perfectly plastic. During the rocking motion of slender blocks, if additional energy is lost because of interface mechanisms, the value of the true coefficient of restitution r will be less than the one computed from (15).

Condition for Sustaining Rocking Motion

When the block is rocking, the horizontal and vertical reactions at points O or O' fluctuate with time. Dynamic equilibrium in the horizontal and vertical directions gives

$$f_x(t) = m(\ddot{x}(t) + \dot{x}(t)) \quad (16)$$

$$f_z(t) = m(g + \ddot{z}(t)) \quad (17)$$

where $x(t)$ and $z(t)$ = horizontal and vertical displacements of the center of mass of the block. The kinematics of the rocking motion yields that

$$\ddot{x}(t) = R\ddot{\theta}(t)\cos[\alpha \text{sgn}[\theta(t)] - \theta(t)] + R\dot{\theta}(t)^2 \sin[\alpha \text{sgn}[\theta(t)] - \theta(t)] \quad (18)$$

$$\ddot{z}(t) = R\ddot{\theta}(t)\sin[\alpha \text{sgn}[\theta(t)] - \theta(t)] - R\dot{\theta}(t)^2 \cos[\alpha \text{sgn}[\theta(t)] - \theta(t)] \quad (19)$$

and $\dot{\theta}(t)$ = angular velocity of the block; and $\ddot{\theta}(t)$ = angular acceleration of the block that is given by (12). Eqs. (18) and (19) can also be found in the paper by Pompei et al. (1998). The substitution of (16) and (17) into (9) in association with (12), (18), and (19) gives that the condition needed to avoid sliding during the entire rocking motion is

$$\left| \frac{f_x(t)}{f_z(t)} \right| = \left| \left\{ \frac{\ddot{u}_g}{g} (5 - 3 \cos 2[\alpha \text{sgn}[\theta] - \theta]) - 3 \sin 2[\alpha \text{sgn}[\theta] - \theta] + 6 \frac{\dot{\theta}^2}{p^2} \sin[\alpha \text{sgn}[\theta] - \theta] \right\} / \left\{ 5 - 3 \frac{\ddot{u}_g}{g} \sin 2[\alpha \text{sgn}[\theta] - \theta] + 3 \cos 2[\alpha \text{sgn}[\theta] - \theta] - 6 \frac{\dot{\theta}^2}{p^2} \cos[\alpha \text{sgn}[\theta] - \theta] \right\} \right| < \mu \quad (20)$$

The reader can easily verify that, under a one-sine pulse at the instant when rocking initiates ($t = 0$), $\ddot{u}_g(0) = g \tan \alpha$ and $\dot{\theta}(0) = 0$. With these initial conditions, (20) reduces to (8), which is the traditional expression that one derives from static analysis.

The response of a free-standing block subjected to various horizontal cycloidal pulses with frequency ω_p —such as a one-sine pulse (Type-A pulse), one-cosine pulse (Type-B pulse), and pulses with n cycles in their displacement histories (Type- C_n pulses)—was investigated in recent studies by Makris and Roussos (1998, 2000). Those studies were motivated by an

increasing number of ground motions, recorded near the source of strong earthquakes, that contain one or more relatively long-duration coherent pulses. In view of the relatively long duration of the coherent pulses, the range of interest in the frequency ratio, ω_p/p , for electrical equipment $p \approx 2$ rad/s is $0 \leq \omega_p/p \leq 3$. Within this range of excitation frequencies ($0 \leq \omega_p/p \leq 3$), the minimum overturning acceleration spectrum of cycloidal pulses is nearly linear. Makris and Roussos (1998, 2000) proposed the approximate expression

$$\frac{a_{p0}}{\alpha g} \approx 1 + \beta \frac{\omega_p}{p} \quad (21)$$

where a_{p0} = minimum overturning acceleration of the pulse; and α = angle of the block slenderness. The coefficient $\beta = 1/6$ for Type-A or Type-C_n pulses, and $\beta = 1/4$ for a Type-B pulse. For values of $\omega_p/p \geq 3$, the minimum overturning acceleration spectra become increasingly nonlinear. Although the range of $\omega_p/p \geq 3$ is not of central interest in evaluating the overturning potential of long period motions, it is of prime interest when the overturning of a block is the result of a high-frequency spike with short duration.

ROCKING RESPONSE UNDER ONE-SINE (TYPE-A) PULSE

The analysis presented in this section concentrates on the overturning potential of a one-sine pulse shown in 4 (left) with ground acceleration

$$\ddot{u}_g(t) = a_p \sin(\omega_p t + \psi), \quad -\psi/\omega_p \leq t \leq (2\pi - \psi)/\omega_p \quad (22a)$$

$$\ddot{u}_g(t) = 0, \quad \text{otherwise} \quad (22b)$$

where $\psi = \sin^{-1}(\alpha g/a_p)$ = phase angle when rocking initiates. At this instant, $\ddot{u}_g(0) = \alpha g = \lambda a_p$, and, according to (8), the condition for the block to enter pure rocking is $\tan \alpha = (b/h) < \mu$. However, to maintain pure rocking motion during the entire excitation, the minimum values of the coefficient of friction are bounded by (20). For tall, slender blocks, the angle $\alpha = \text{atan}(b/h)$ is relatively small and (10) and (11) can be linearized.

Anooshehpour et al. (1999) attempted to construct the minimum overturning acceleration spectra due to a one-sine pulse by considering the linear approximation. Their study was motivated from the temptation to estimate peak ground acceleration at Point Reyes, Calif., during the 1906 San Francisco earthquake. Unfortunately, their study ignored the presence of the second mode of overturning (without impact), which further complicates the dynamics of the response, and they overlooked the sensitivity of the response to the nonlinear nature of the problem. In this section the correct minimum overturning acceleration spectra of a free-standing block subjected to a one-sine pulse are computed: (1) by adopting the linear approximation; and (2) by considering the fully nonlinear nature of the problem.

Linear Formulation

Within the limits of the linear approximation and for a horizontal ground acceleration given by (22), (10) and (11) become

$$\ddot{\theta}(t) - p^2\theta(t) = -\frac{a_p}{g} p^2 \sin(\omega t + \psi) + p^2\alpha, \quad \theta < 0 \quad (23)$$

$$\ddot{\theta}(t) - p^2\theta(t) = -\frac{a_p}{g} p^2 \sin(\omega t + \psi) - p^2\alpha, \quad \theta > 0 \quad (24)$$

The integration of (23) and (24) gives

$$\begin{aligned} \theta(t) &= A_1 \sinh(pt) + A_2 \cosh(pt) - \alpha \\ &+ \frac{1}{1 + \frac{\omega_p^2}{p^2}} \frac{a_p}{g} \sin(\omega_p t + \psi), \quad \theta < 0 \end{aligned} \quad (25)$$

$$\begin{aligned} \theta(t) &= A_3 \sinh(pt) + A_4 \cosh(pt) + \alpha \\ &+ \frac{1}{1 + \frac{\omega_p^2}{p^2}} \frac{a_p}{g} \sin(\omega_p t + \psi), \quad \theta > 0 \end{aligned} \quad (26)$$

where

$$A_1 = A_3 = \frac{\dot{\theta}_0}{p} - \frac{\omega_p/p}{1 + \omega_p^2/p^2} \frac{a_p}{g} \cos(\psi) = \frac{\dot{\theta}_0}{p} - \alpha \frac{\omega_p/p}{1 + \omega_p^2/p^2} \frac{\cos(\psi)}{\sin(\psi)} \quad (27)$$

$$A_2 = \theta_0 + \alpha - \frac{1}{1 + \omega_p^2/p^2} \frac{a_p}{g} \sin(\psi) = \theta_0 + \alpha - \frac{\alpha}{1 + \omega_p^2/p^2} \quad (28)$$

$$A_4 = \theta_0 - \alpha - \frac{1}{1 + \omega_p^2/p^2} \frac{a_p}{g} \sin(\psi) = \theta_0 - \alpha - \frac{\alpha}{1 + \omega_p^2/p^2} \quad (29)$$

The time histories for the angular velocities are directly obtained from the time derivatives of (25) and (26)

$$\begin{aligned} \dot{\theta}(t) &= pA_1 \cosh(pt) + pA_2 \sinh(pt) \\ &+ \frac{\omega_p}{1 + \frac{\omega_p^2}{p^2}} \frac{a_p}{g} \cos(\omega_p t + \psi), \quad \theta < 0 \end{aligned} \quad (30)$$

$$\begin{aligned} \dot{\theta}(t) &= pA_3 \cosh(pt) + pA_4 \sinh(pt) \\ &+ \frac{\omega_p}{1 + \frac{\omega_p^2}{p^2}} \frac{a_p}{g} \cos(\omega_p t + \psi), \quad \theta > 0 \end{aligned} \quad (31)$$

The solutions given by (25) and (26) can be pieced together to construct the time history of the rocking response under a given acceleration amplitude a_p . Furthermore, this solution can yield the minimum overturning acceleration amplitude, provided that a condition of overturning is available.

Under the minimum acceleration amplitude, blocks overturn during their free-vibration regime at a theoretically infinite large time when the velocity tends to reach a local minimum (Makris and Roussos 1998). Accordingly the condition for overturning is that

$$\dot{\theta}(t_\infty) = 0 \quad (32)$$

where t_∞ = sufficiently large time, where $\tanh(pt_\infty) = 1$.

Under a one-sine pulse, a free-standing block has two modes of overturning: (1) overturning with one impact (mode 1); and (2) overturning with no impact (mode 2). This result is true as long as ω_p/p is sufficiently small. As ω_p/p increases, the first mode of impact vanishes and the block overturns only without impact (mode 2). Accordingly, to back-figure the minimum overturning acceleration amplitude by imposing the condition of overturning given by (32), one has to distinguish between modes 1 and 2.

Mode 1

Denoting the time as t_{f_1} when the block enters its free-vibration regime, the condition for overturning after the block has experienced one impact (mode 1) is

$$\dot{\theta}(t_{f_1}) + p[\theta(t_{f_1}) - \alpha] = 0 \quad (33)$$

In the case where the impact happens before the excitation expires ($t_i < T_{ex}$), $t_{fv} = T_{ex} = (2\pi - \psi)/\omega_p$ (case 1). In the case where the impact happens after the excitation expires ($t_i > T_{ex}$), $t_{fv} = t_i$ (case 2).

Case 1 ($t_i < T_{ex}$). In this case the condition of overturning given by (32) yields

$$\dot{\theta}(T_{ex}) + p[\theta(T_{ex}) - \alpha] = 0 \quad (34)$$

where

$$\begin{aligned} \theta(T_{ex}) = & A_3 \sinh[p(T_{ex} - t_i)] + A_4 \cosh[p(T_{ex} - t_i)] + \alpha \\ & + \frac{a_p/g}{1 + \left(\frac{\omega_p}{p}\right)^2} \sin(\omega_p T_{ex} + \psi) \end{aligned} \quad (35)$$

$$\begin{aligned} \dot{\theta}(T_{ex}) = & pA_3 \cosh[p(T_{ex} - t_i)] + pA_4 \sinh[p(T_{ex} - t_i)] \\ & + \frac{\omega_p(a_p/g)}{1 + \left(\frac{\omega_p}{p}\right)^2} \cos(\omega_p T_{ex} + \psi) \end{aligned} \quad (36)$$

The integration constants A_3 and A_4 are given by

$$A_3 = \frac{\eta \dot{\theta}^{\text{before}}(t_i)}{p} - \frac{\omega_p/p}{1 + \left(\frac{\omega_p}{p}\right)^2} \frac{a_p}{g} \cos(\omega_p t_i + \psi) \quad (37)$$

$$A_4 = -\alpha - \frac{1}{1 + \left(\frac{\omega_p}{p}\right)^2} \frac{a_p}{g} \sin(\omega_p t_i + \psi) \quad (38)$$

where η = coefficient of restitution. The time of impact t_i is related to the acceleration amplitude, $a_p = \alpha g / \sin \psi$, with the expression

$$\tan \psi = \frac{\sin(\omega_p t_i) - \frac{\omega_p}{p} \sinh(pt_i)}{1 + \left(\frac{\omega_p}{p}\right)^2 - \left(\frac{\omega_p}{p}\right)^2 \cosh(pt_i) - \cos(\omega_p t_i)} \quad (39)$$

The condition of overturning given by (34) takes the form

$$(A_3 + A_4) \exp[p(T_{ex} - t_i)] + \frac{\omega_p/p}{1 + \left(\frac{\omega_p}{p}\right)^2} \frac{a_p}{g} = 0 \quad (40)$$

where A_3 and A_4 are given by (37) and (38); and t_i = solution of (39). The value of $a_p/(\alpha g)$ that satisfies (40) is the minimum overturning acceleration. Eq. (40) is valid when $t_i \leq T_{ex}$. Within the limits of the linear approximation (slender block) and assuming a value of $\eta = 0.9$, this happens when $0 \leq \omega_p/p \leq 4.8$.

Case 2 ($t_i > T_{ex}$). In this case the condition of overturning yields

$$\dot{\theta}^{\text{after}}(t_i) - p\alpha = 0 \quad (41)$$

where $\dot{\theta}^{\text{after}}(t_i) = \eta \dot{\theta}^{\text{before}}(t_i)$, and

$$\begin{aligned} \dot{\theta}^{\text{before}}(t_i) = & \frac{\alpha \omega_p}{1 + \frac{\omega_p^2}{p^2}} \left[\frac{1}{\sin \psi} - \frac{\cosh(pT_{ex})}{\tan \psi} + \frac{\omega_p}{p} \sinh(pT_{ex}) \right] \\ & \cdot \cosh[p(t_i - T_{ex})] + \frac{\alpha \omega_p}{1 + \frac{\omega_p^2}{p^2}} \left[-\frac{\sinh(pT_{ex})}{\tan \psi} + \frac{\omega_p}{p} \cosh(pT_{ex}) \right] \\ & \cdot \sinh[p(t_i - T_{ex})] \end{aligned} \quad (42)$$

In the above equations, the impact time t_i is the solution of the transcendental equation

$$\begin{aligned} g(t_i, \psi) = & \frac{\alpha(\omega_p/p)}{1 + (\omega_p/p)^2} \left(\left[\frac{1}{\sin \psi} - \frac{\cosh(pT_{ex})}{\tan \psi} + \frac{\omega_p}{p} \sinh(pT_{ex}) \right] \right. \\ & \cdot \sinh[p(t_i - T_{ex})] + \left[-\frac{\sinh(pT_{ex})}{\tan \psi} + \frac{\omega_p}{p} \cosh(pT_{ex}) \right] \\ & \left. \cdot \cosh[p(t_i - T_{ex})] - \alpha \right) = 0 \end{aligned} \quad (43)$$

The simultaneous solution of (41) and (43) gives the minimum overturning acceleration for the case $t_i > T_{ex}$.

Mode 2

Under this mode, the block does not experience any impact. The condition of overturning becomes

$$\frac{\dot{\theta}(T_{ex})}{p} + [\theta(T_{ex}) + \alpha] = 0 \quad (44)$$

where

$$\dot{\theta}(T_{ex}) = \frac{\alpha(\omega_p/p)}{1 + (\omega_p/p)^2} \left[-\frac{\sinh(pT_{ex})}{\tan \psi} + \frac{\omega_p}{p} \cosh(pT_{ex}) \right] - \alpha \quad (45)$$

$$\theta(T_{ex}) = \frac{\alpha \omega_p}{1 + (\omega_p/p)^2} \left[-\frac{\cosh(pT_{ex})}{\tan \psi} + \frac{\omega_p}{p} \sinh(pT_{ex}) + \frac{1}{\sin \psi} \right] \quad (46)$$

The substitution of (45) and (46) into (44) leads to

$$\frac{\omega_p}{p} \sin \psi - \cos \psi = -\exp \left[\frac{p}{\omega_p} (2\pi - \psi) \right] \quad (47)$$

The solution of (47) gives the minimum acceleration amplitude that is capable of overturning the block without any impact. Fig. 6 plots the solutions of the condition of overturning (for $\eta = 0.9$) after distinguishing carefully between modes 1 and 2 of overturning. Although the roots are computed numerically, this solution is referred to as an analytical solution because it is based on the analytical expressions of the response given by (25) and (26).

Fig. 6 indicates that, when ω_p/p is sufficiently small, the minimum overturning acceleration is the result of mode 1. Overturning with mode 2 may also happen; however, a much higher acceleration amplitude is needed to manifest it. The distinction between modes 1 and 2 of overturning is of particular interest, because the transition from overturning with one impact to overturning without impact is not immediate and there is a finite margin of acceleration amplitudes with magnitudes larger than the minimum overturning acceleration (that corresponds to mode 1) that are unable to overturn the block. This interesting behavior, illustrated in Figs. 7 and 8, shows response time histories of a free-standing block with $p = 2.14$ rad/s, $\alpha = 0.25$ rad, $\eta = 0.9$, and $\omega_p/p = 5$ for various levels of the amplitude a_p of the acceleration pulse.

The left and center plots in Fig. 7 show normalized rotations and angular velocity histories at the verge of overturning because of the first (minimum) level of the acceleration amplitude. With $a_p = 3\alpha g$, the block does not overturn, whereas when $a_p = 3.01\alpha g$, the block overturns after experiencing one impact (mode 1). In this case the impact happens after the expiration of the pulse. A similar pattern of overturning prevails until the acceleration amplitude reaches $a_p = 6.32\alpha g$. A notable difference, shown in the right plots, is that, although the first maximum positive rotation θ exceeds α , the decelerating motion of the ground is capable of recentering the block, which will experience an impact considerably later and eventually will overturn.

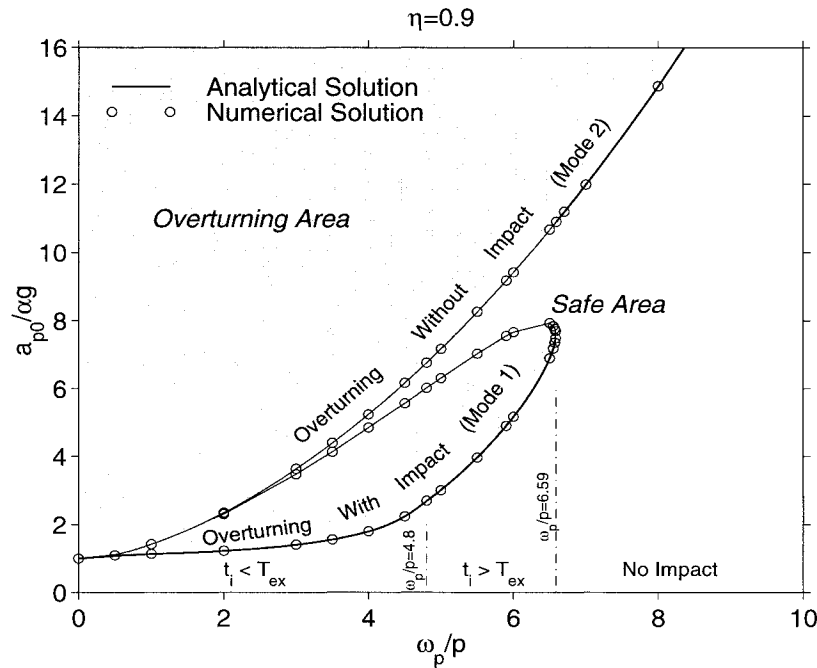


FIG. 6. Overturning Acceleration Spectrum of Free-Standing Block with $\eta = 0.9$ Subjected to One-Sine Acceleration Pulse with Frequency ω_p (Both Analytical and Numerical Solutions Shown Are Computed with Linear Formulation)

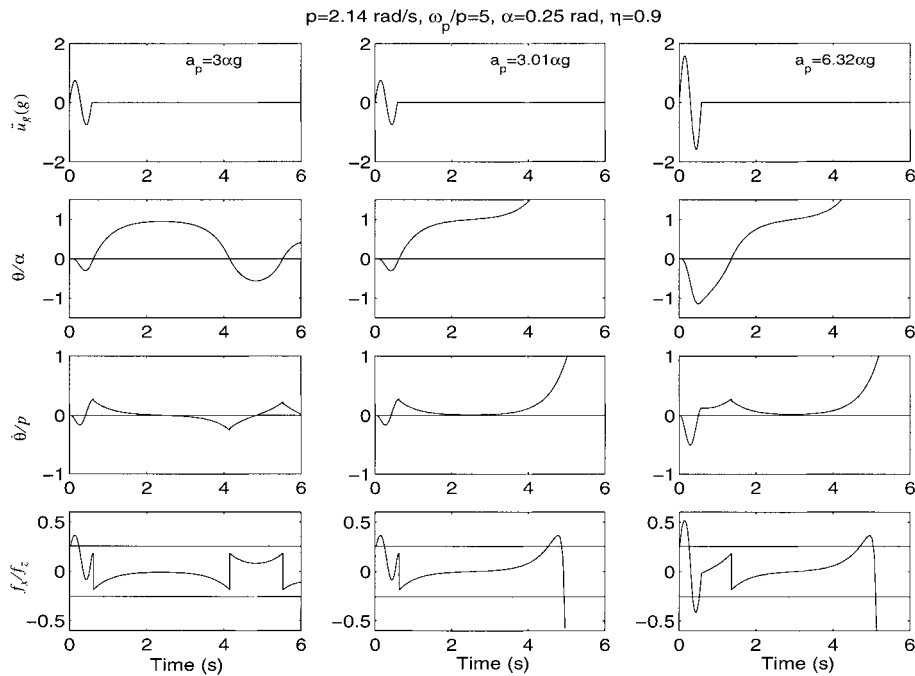


FIG. 7. Rotation, Angular Velocity, and Horizontal-to-Vertical Reaction Time Histories of Rigid Block ($p = 2.14$ rad/s, $\alpha = 0.25$ rad, and $\eta = 0.9$) Subjected to One-Sine Pulse with $\omega_p/p = 5$ [Left: $a_p = 3.00\alpha g$, No Overturning; Center: $a_p = 3.01\alpha g$, Overturning with One Impact (Mode 1); Right: $a_p = 6.32\alpha g$, Overturning with One Impact (Mode 1)]

Fig. 8 (left) shows the response of the same free-standing block when the acceleration amplitude of the one-sine pulse has been slightly increased, $a_p = 6.33\alpha g$. Interestingly, the block does not overturn. This finding is because the acceleration pulse is intense enough to induce such a large rotation that the block escapes most of the overturning effect of the decelerating portion of the excitation pulse. This beneficial arrangement between inertia and gravity forces holds until $a_p = 7.17\alpha g$, as shown in the center of Fig. 8. Eventually, if the acceleration amplitude a_p is further increased, the block will overturn without experiencing any impact (mode 2), as shown

in Fig. 8 (right). It should be noted that Yim et al. (1980) have reported the situation where a free-standing block topples under a certain level of a given ground motion, yet it does not topple when the acceleration of the same ground motion is further increased. Figs. 7 and 8, in association with the foregoing discussion, elucidate this counterintuitive result.

Accordingly, in the frequency-acceleration plane, there is a safe area that extends above the minimum overturning acceleration boundary due to mode 1 of overturning. When $0 < \omega/p \leq 6.59$, ($\eta = 0.9$), the minimum overturning acceleration is the result of mode 1 (one impact). With reference to Fig. 6,

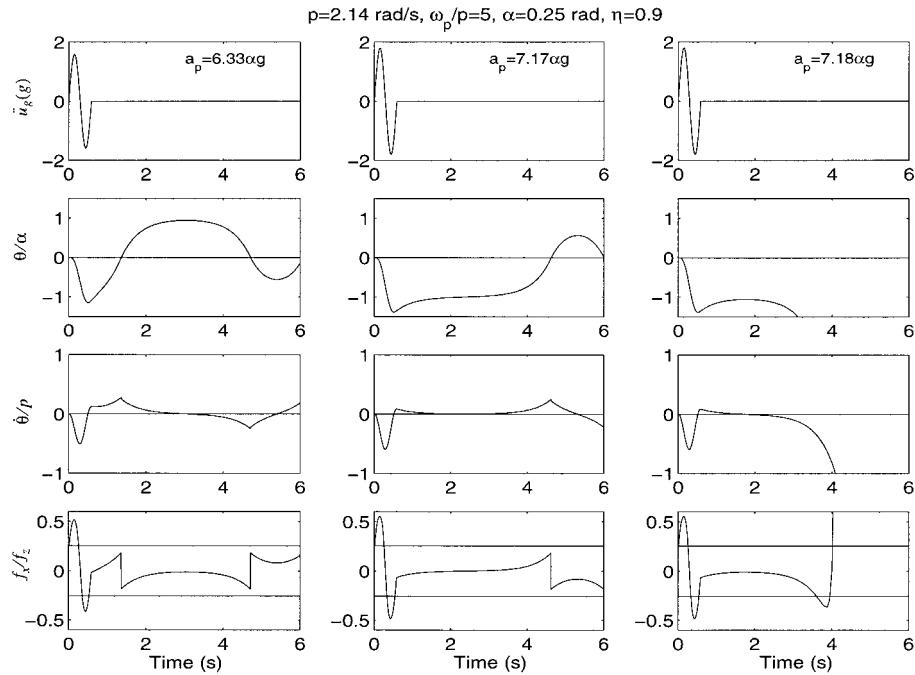


FIG. 8. Rotation, Angular Velocity, and Horizontal-to-Vertical Reaction Time Histories of Same Rigid Block as in Fig. 7 Subjected to One-Sine Pulse with $\omega_p/p = 5$ [Left: No Overturning with $a_p = 6.33\alpha g$, That Is, Slightly Larger Than Acceleration Level, $a_p = 6.32\alpha g$, That Created Overturning; Center: Block Does Not Overturn Even for Acceleration Amplitude $a_p = 7.17\alpha g$; Right: Block Eventually Overturns with $a_p = 7.18\alpha g$, without Impact (Mode 2)]

when $\omega/p > 6.59$, blocks overturn only with mode 2 (no impact) and a substantial increase in the acceleration amplitude is needed to create overturning.

To further validate these results, the various overturning boundaries were computed numerically by means of a state-space formulation that were developed to account for the nonlinear nature of the problem. With reference to (23) and (24), the state vector of the system is merely

$$\{y(t)\} = \begin{Bmatrix} \theta(t) \\ \dot{\theta}(t) \end{Bmatrix} \quad (48)$$

and the time-derivative vector $\mathbf{f}(t)$ is

$$\mathbf{f}(t) = \{ \dot{y}(t) \} = \begin{Bmatrix} \dot{\theta}(t) \\ -p^2 \left[\sin[\alpha \operatorname{sgn}[\theta(t)] - \theta(t)] + \frac{\ddot{u}_g}{g} \cos[\alpha \operatorname{sgn}[\theta(t)] - \theta(t)] \right] \end{Bmatrix} \quad (49)$$

For slender blocks, the linear approximation becomes dependable and (49) reduces to

$$\mathbf{f}(t) = \{ \dot{y}(t) \} = \begin{Bmatrix} \dot{\theta}(t) \\ p^2 \left[-\alpha \operatorname{sgn}[\theta(t)] + \theta(t) - \frac{\ddot{u}_g(t)}{g} \right] \end{Bmatrix} \quad (50)$$

The numerical integration of (49) or (50) is performed with standard Ordinary Differential Equation (ODE) solvers available in MATLAB (*High-performance* 1992). The result of the numerical solution of (50), shown in Fig. 6 with circles, are in excellent agreement with the analytical solution.

The bottom plots in Figs. 7 and 8 show the time history of the ratio given by (20) for the case $p = 2.14$ rad/s, $\alpha = 0.25$ rad, and $\omega_p/p = 5$. Although at the initiation of rocking ($t = 0$), $f_x(0)/f_z(0) = \tan \alpha \approx 0.25$ for all acceleration levels, the

ratio of the horizontal to vertical force later exceeds the slenderness of the block. This increase is a function of the amplitude of the input pulse. Fig. 9 (top) plots the minimum value of the coefficient of friction needed to sustain pure rocking motion during the entire duration of a one-sine (Type-A) pulse as a function of the amplitude of the pulse, for $\alpha = 0.25$ rad and three cases of ω_p/p . For each case of ω_p/p , the values shown in Fig. 9 were extracted by computing the rocking time histories until the blocks overturned with mode 2. The values shown in Fig. 9 have been computed with the nonlinear formulation.

Nonlinear Formulation

Fig. 10 (top) plots with crosses the overturning acceleration spectra of a rigid block with $\alpha = 0.25$ rad, $p = 2.14$ rad/s, and $\eta = 0.9$, where the various overturning boundaries are computed numerically with the nonlinear formulation expressed with (49). The aforementioned rigid block parameters are those associated with the locomotive shown in Fig. 2. The circles shown in Fig. 10 are the results computed with the linear formulation expressed by (50). Note that, although for values of ω_p/p up to 6, the linear approximation gives equally good results as the nonlinear formulation, for $6 \leq \omega_p/p \leq 7.58$, the two formulations give drastically different results. As an example, under a one-sine pulse with $\omega_p = 15.7$ rad/s ($f = 2.5$ Hz), the linear formulation yields that the locomotive with $\alpha = 0.25$ rad, $p = 2.14$ rad/s, and $\eta = 0.9$ will overturn under a minimum acceleration amplitude, $a_{p0} = 3.24g$ due to mode 2 whereas the nonlinear formulation yields an overturning acceleration amplitude $a_{p0} = 2.22g$ due to mode 1. This drastic difference is because, under the nonlinear formulation, the overturning “bay” penetrates further into the safe area. These drastic differences disappear for pulse frequencies beyond 2.58 Hz, because according to both formulations, the free-standing block overturns with mode 2 (no impact). Accordingly the results obtained with the linear formulation should be used with caution. To conclude this example, according to a witness testimony reported by Anooshehpour et al. (1999), the loco-

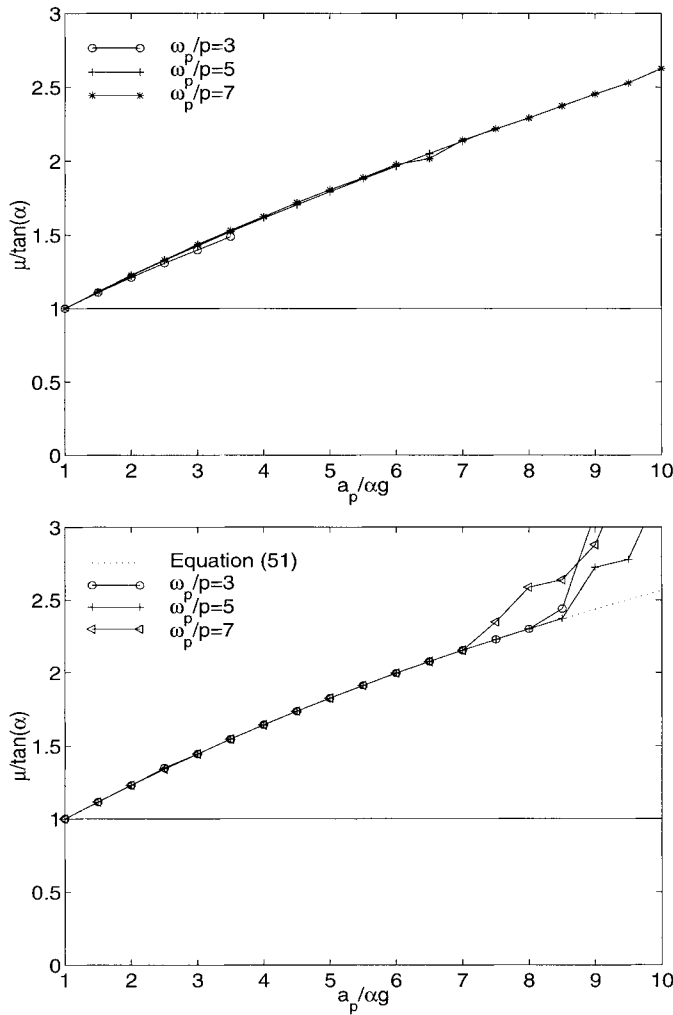


FIG. 9. Normalized Minimum Coefficient of Friction over Slenderness of Block That Is Needed to Sustain Pure Rocking Motion under One-Sine Pulse (Top) and One-Cosine Pulse (Bottom)

motive apparently overturned with mode 1. As is shown in this nonlinear analysis, mode 1 can exist even under excitation frequencies as high as $f = 2.5$ Hz. Assuming the locomotive overturned because of 15.7 rad/s one-sine pulse with amplitude $a_p/(\alpha g) = 2.22/0.25 \approx 8.9$, Fig. 9(top) indicates that the coefficient of friction needed to sustain the rocking motion is approximately $\mu = 2.5 \tan \alpha = 0.625$. Although a coefficient of friction $\mu = 0.625$ seems to be high, in the case of the locomotive shown in Fig. 2, the sliding mode was prevented because the wheels engage on the tracks and the sole rigid-body mode of motion is the rocking mode. This implies that the possibility that the locomotive toppled because of an unusually high ground acceleration ($\ddot{u}_g \approx 2.0g$) should not be excluded.

The existence of the safe “cape” that embraces the overturning “bay,” and the sensitivity of the response to the nonlinear nature of the problem even for blocks as slender as a train locomotive ($\alpha = 0.25$ rad = 14.32°), complicates the problem of estimating ground motions by only observing objects that either toppled or survived a historic earthquake.

Fig. 10 (bottom) plots overturning acceleration spectra of a rigid equipment with $\alpha = 0.349$ rad = 20°, $p = 2.0$ rad/s, and $\eta = \sqrt{r_{\max}} \approx 0.825$. The crosses are the result of the nonlinear formulation, whereas the circles are the results computed with a linear formulation. Again, within the low range of ω_p/p , the linear formulation gives equally good results as the nonlinear formulation. However, within the range $4.7 \leq \omega_p/p \leq 5.8$, the two formulations give drastically different results.

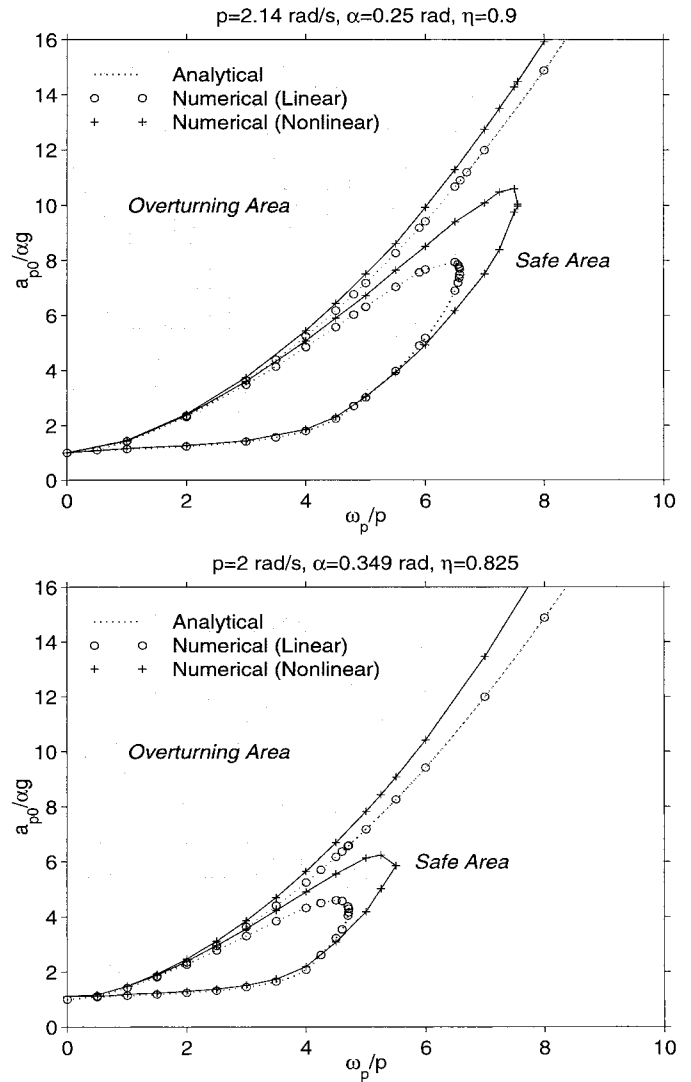


FIG. 10. Comparison of Overturning Acceleration Spectra of Slender Block under One-Sine Pulse Computed with Linear and Nonlinear Formulation

ROCKING RESPONSE UNDER ONE-COSINE (TYPE-B) PULSE

Whereas a one-sine acceleration pulse results in a forward ground displacement, a one-cosine acceleration pulse results in a forward-and-back ground displacement. With reference to Fig. 4 (right), under a one-cosine acceleration pulse, the maximum ground acceleration is induced at the instant when rocking initiates ($\lambda = 1$) and the condition for the block to enter rocking motion without sliding given by (7) becomes

$$\tan \alpha \cdot \frac{\frac{a_p}{g \sin \alpha} - \frac{3}{4} \cos \alpha \left(\frac{a_p}{g \tan \alpha} - 1 \right)}{\frac{\tan \alpha}{\sin \alpha} + \frac{3}{4} \tan \alpha \sin \alpha \left(\frac{a_p}{g \tan \alpha} - 1 \right)} < \mu \quad (51)$$

while for slender blocks ($\sin \alpha \approx \tan \alpha \approx \alpha$ and $\cos \alpha \approx 1$) simplifies to

$$\alpha \cdot \frac{\frac{3}{4} + \frac{1}{4} \frac{a_p}{\alpha g}}{1 + \frac{3}{4} \alpha^2 \left(\frac{a_p}{\alpha g} - 1 \right)} < \mu \quad (52)$$

Eq. (51), or its slender-block approximation given by (52), indicates that, the stronger the acceleration amplitude of a

Type-B pulse, the larger needs to be the static coefficient of friction in order for the block to enter rocking motion. This is in contrast with a Type-A pulse, where the condition for a block to enter rocking motion is independent of the acceleration level ($\tan \alpha < \mu$). Furthermore, to sustain rocking motion during the entire duration of a Type-B pulse, (20) needs to be satisfied. Fig. 9 (bottom) plots the minimum value of the coefficient of friction needed to sustain pure rocking motion during the entire duration of a one-cosine (Type-B) pulse as a function of the amplitude of the pulse, $a_p/(\alpha g)$ for $\alpha = 0.25$. In addition, the minimum value of the coefficient of friction needed for the block to enter rocking motion that is computed with the static expression given by (51) is shown and it is observed that it captures with fidelity the results obtained with the dynamic formulation. As an example, Fig. 9 (bottom) indicates that when a free-standing block with $\alpha = 0.25$ is subjected to a Type-B pulse with $a_p/(\alpha g) \approx 6$, the minimum coefficient of friction needed to sustain pure rocking is approximately two times the value of the block slenderness.

Fig. 11 plots the overturning acceleration spectra due to a one-cosine acceleration pulse with time history

$$\ddot{u}_g(t) = a_p \cos(\omega_p t), \quad 0 < t < 2\pi/\omega_p \quad (53a)$$

$$\ddot{u}_g(t) = 0, \quad \text{otherwise} \quad (53b)$$

The same rigid block with the parameters of the locomotive shown in Fig. 2 ($\alpha = 0.25$ rad, $p = 2.14$ rad/s, and $\eta = 0.9$) is considered. The circles, shown in Fig. 11 (top), are the results computed with the linear formulation, whereas the crosses are the results obtained with the nonlinear formulation. In this case the differences observed between the linear and

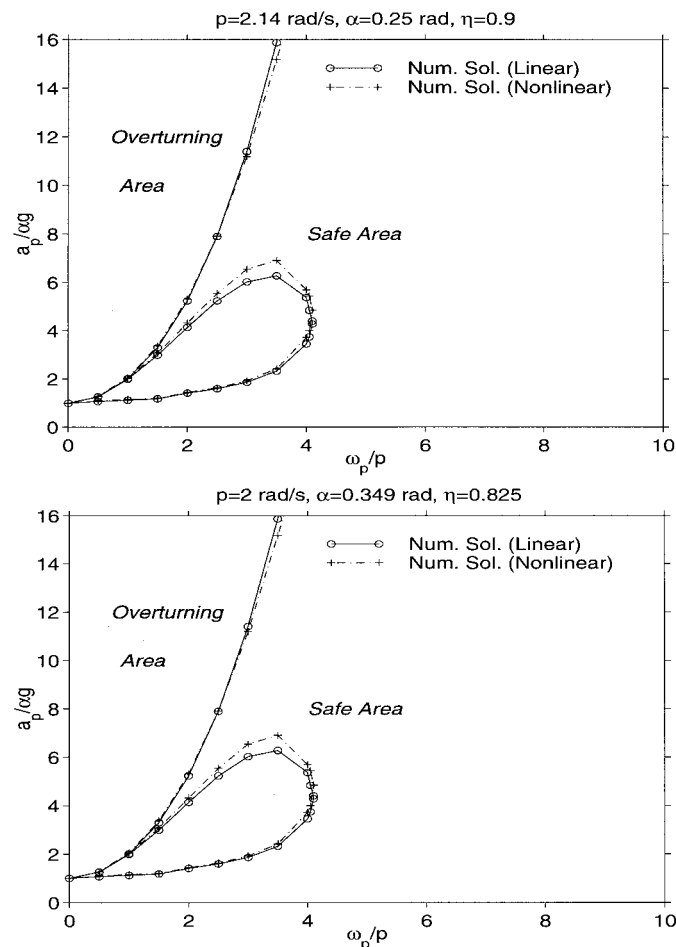


FIG. 11. Comparison of Overturning Acceleration Spectra of Slender Block under One-Cosine Pulse Computed with Linear and Nonlinear Formulation

the nonlinear formulation are less drastic. Fig. 11 (top) indicates that, under a one-cosine pulse with frequency ω_p , blocks that are small enough, $\omega_p/p \leq 4$, can experience two distinct modes of overturning. Again, the existence of these two modes are responsible for the generation of a safe region that embraces the minimum overturning acceleration spectrum. Consequently, similar to the case of one-sine pulse, there is a finite margin of acceleration amplitudes with magnitudes larger than the minimum overturning acceleration (which corresponds to mode 1) that are unable to overturn the block. Fig. 11 (bottom) plots overturning acceleration spectra under a one-cosine pulse of a rigid equipment with $\alpha = 0.349$ rad = 20° , $p = 2.0$ rad/s, and $\eta = \sqrt{r_{\max}} = 0.825$. The crosses are the result of the nonlinear formulation, whereas the circles are the results computed with the linear formulation. In comparing Fig. 11 (top) with Fig. 11 (bottom), one concludes that the normalized overturning acceleration spectra have a mild dependence on the slenderness of the block α and the frequency parameter p .

CONCLUSIONS

This paper revisits the rocking motion and overturning of a free-standing block subjected to cycloidal pulses. The dynamic interface forces that develop during rocking motion are derived, and it is shown that the level of the friction coefficient needed to sustain rocking motion during the entire duration of the pulse is an increasing function of the acceleration level of the pulse.

This paper reveals that, under cycloidal pulses, a free-standing block can overturn with two distinct modes: (1) by exhibiting one or more impacts; and (2) without exhibiting any impact. The existence of the second mode results in a safe region that is located on the acceleration-frequency plane over the minimum overturning acceleration spectrum. This safe region contains acceleration amplitudes with magnitudes larger than the minimum overturning acceleration (which corresponds to mode 1) and are unable to overturn the block. It is found that the shape of this region depends on the coefficient of restitution and is sensitive to the nonlinear nature of the problem. The transition from mode 1 to mode 2 is sudden and results in a finite jump in the minimum overturning acceleration spectrum. This paper concludes that the sensitive nonlinear nature of the problem, in association with the presence of the safe region that embraces the minimum overturning acceleration spectrum, complicates further the task of estimating the peak ground acceleration by only examining the geometry of free-standing objects that either overturned or survived a ground shaking.

ACKNOWLEDGMENTS

This work is supported by the Pacific Gas and Electric Co. under Grant PG&E-UCB-00956 to the Pacific Earthquake Engineering Center, University of California, Berkeley.

REFERENCES

- Anooshehpour, A., Heaton, T. H., Shi, B., and Brune, J. N. (1999). "Estimates of the ground acceleration at Point Reyes station during the 1906 San Francisco earthquake." *Bull. Seismological Soc. of Am.*, 89(4), 843–853.
- Aslam, M., Scalise, D. T., and Godden, W. G. (1980). "Earthquake rocking response of rigid bodies." *J. Struct. Div.*, ASCE, 106(2), 377–392.
- Campillo, M., Gariel, J. C., Aki, K., and Sanchez-Sesma, F. J. (1989). "Destructive strong ground motion in Mexico City: Source, path and site effects during the great 1985 Michoagan earthquake." *Bull. Seismological Soc. of Am.*, 79(6), 1718–1735.
- High-performance numeric computation and visualization software.* (1992). MathWorks, Natick, Mass.
- Hogan, S. J. (1989). "On the dynamics of rigid-block motion under harmonic forcing." *Proc., Royal Soc.*, London, A425, 441–476.
- Hogan, S. J. (1990). "The many steady state responses of a rigid block

- under harmonic forcing." *Earthquake Engrg. and Struct. Dyn.*, 19(7), 1057–1071.
- Housner, G. W. (1963). "The behaviour of inverted pendulum structures during earthquakes." *Bull. Seismological Soc. of Am.*, 53(2), 404–417.
- Iwan, W. D., and Chen, X. D. (1994). "Important near-field ground motion data from the Landers earthquake." *Proc., 10th Eur. Conf. Earthquake Engrg.*, Balkema, Rotterdam, The Netherlands.
- Jacobsen, L. S., and Ayre, R. S. (1958). *Engineering vibrations*, McGraw-Hill, New York.
- Makris, N., and Roussos, Y. (1998). "Rocking response and overturning of equipment under horizontal pulse-type motions." *Rep. No. PEER-98/05*, Pacific Earthquake Engrg. Res. Ctr., University of California, Berkeley, Calif.
- Makris, N., and Roussos, Y. (2000). "Rocking response of rigid blocks under near-source ground motions." *Géotechnique*, London, 50(3), 243–262.
- Pompei, A., Scalia, A., and Sumbatyan, M. A. (1998). "Dynamics of rigid block due to horizontal ground motion." *J. Engrg. Mech.*, ASCE, 124(7), 713–717.
- Scalia, A., and Sumbatyan, M. A. (1996). "Slide rotation of rigid bodies subjected to a horizontal ground motion." *Earthquake Engrg. and Struct. Dyn.*, 25, 1139–1149.
- Shenton, H. W., III. (1996). "Criteria for initiation of slide, rock, and slide-rock rigid-body modes." *J. Engrg. Mech.*, ASCE, 122(7), 690–693.
- Shi, B., Anooshehpour, A., Zeng, Y., and Brune, J. N. (1996). "Rocking and overturning of precariously balanced rocks by earthquake." *Bull. Seismological Soc. of Amer.*, 86(5), 1364–1371.
- Spanos, P. D., and Koh, A. S. (1984). "Rocking of rigid blocks due to harmonic shaking." *J. Engrg. Mech.*, ASCE, 110(11), 1627–1642.
- Tso, W. K., and Wong, C. M. (1989a). "Steady state rocking response of rigid blocks Part 1: Analysis." *Earthquake Engrg. and Struct. Dyn.*, 18(1), 89–106.
- Tso, W. K., and Wong, C. M. (1989b). "Steady state rocking response of rigid blocks Part 2: Experiment." *Earthquake Engrg. and Struct. Dyn.*, 18(1), 107–120.
- Yim, C.-S., Chopra, A. K., and Penzien, J. (1980). "Rocking response of rigid blocks to earthquakes." *Earthquake Engrg. and Struct. Dyn.*, 8(6), 565–587.